Quantum mechanical calculations of the rate constant for the $H_2+OH\rightarrow H+H_2O$ reaction: Full-dimensional results and comparison to reduced dimensionality models

Uwe Manthe,[a] Tamar Seideman,[b] and William H. Miller
Department of Chemistry, University of California, and Chemical Sciences Division, Lawrence Berkeley Laboratory, Berkeley, California 94720

(Received 11 May 1994; accepted 10 June 1994)

The cumulative reaction probability is calculated for the $H_2+OH\rightarrow H+H_2O$ reaction in its full (six) dimensionality for total angular momentum $J=0$. The calculation, which should give the (numerically) exact result for the assumed potential energy surface, yields the cumulative reaction probability directly, without having to solve the complete state-to-state reactive scattering problem. Higher angular momenta ($J>0$) were taken into account approximately to obtain the thermal rate constant $k(T)$ over the range $300°<T<700°$. The result deviates significantly from the experimental rate constant, suggesting that the potential energy surface needs to be improved. A systematic series of reduced dimensionality calculations is carried out in order to characterize the behavior and reliability of these more approximate treatments; a comparison of the full dimensional results with previous reduced dimensionality calculations is also made.

I. INTRODUCTION

The most detailed theoretical description of a chemical reaction, i.e., the state-to-state differential scattering cross section at a well defined collision energy, requires that one solves the Schrödinger equation to obtain the S matrix $S_{n_p,n_r}(J,E)$, the state-to-state transition amplitudes as a function of total energy E and total angular momentum J. (n_r and n_p denote reactant and product quantum states, respectively.) All attributes of the reaction can be expressed in terms of the S matrix, from the most detailed cross sections noted above to the least detailed quantity, namely, the thermal rate constant $k(T)$ which resolves neither reactant nor product quantum states. All of the averaging over initial and final quantum states inherent in the definition of the rate constant are conveniently contained in the cumulative reaction probability (CRP),

$$N(E)=\sum_{J=0}^{\infty}(2J+1)\sum_{n_r,n_p}|S_{n_p,n_r}(J,E)|^2, \tag{1}$$

in terms of which the thermally averaged rate constant is given by

$$k(T)=[2\pi\hbar Q_r(T)]^{-1}\int_{-\infty}^{\infty}e^{-E/kT}N(E)dE, \tag{2}$$

where Q_r is the reactant partition function per unit volume. [The microcanonical rate constant, which is usually of most interest for unimolecular reactions, is also given in terms of the CRP,

$$k(E)=[2\pi\hbar\rho_r(E)]^{-1}N(E), \tag{3}$$

where ρ_r is the reactant density of states.] Therefore, if one is interested only in the rate constant itself, it would clearly be desirable to be able to calculate the CRP directly, without having to determine the complete S matrix. The purpose of this paper is to describe such a theoretical approach to the reaction $H_2+OH\rightarrow H+H_2O$. (Some of the results of this work have been reported in an earlier Communication.[1])

Though accurate reactive scattering calculations have been carried out in recent years for several atom–diatom systems, e.g., H_2+H,[2] $F+H_2$,[3] $Cl+HCl$,[4] there are just beginning to be such calculations for four atom systems. The first system studied was the $H_2+CN\rightarrow H+HCN$ reaction.[5] More recently the $H_2+OH\rightarrow H+H_2O$,[6–9] the $OH+CO\rightarrow H+CO_2$[10] and the $Cl+HOD\rightarrow HCl+OD$ reactions[11] have been studied by quantum calculations. In particular the $H_2+OH\rightarrow H+H_2O$ reaction seems to be becoming a benchmark system for the development of theoretical methods. This reaction has also been the subject of a variety of experimental investigation, and is important in modeling atmospheric and combustion processes. In addition to rate constants measurements, more sophisticated experiments have studied the mode selectivity of the reaction process.[12,13]

Most of the theoretical treatments of the titled reaction to date have involved "reduced dimensionality" approximations. Wang and Bowman[6] developed a model for the $H_2+OH\rightarrow H+H_2O$ reaction where the three distances are included exactly in a 3D-scattering calculation. The remaining three angles are treated in an adiabatic approximation. Clary[7] introduced a rotating bond approximation, effectively reducing the scattering calculation to three dimensional with the H_2 distance, the H_2–OH distance, and the OH rotation included exactly. In a more recent calculation[8] the H_2 rotation was also included exactly, resulting in a four-dimensional full-scattering calculation. Differences from the original three-dimensional treatment were found to be rather small. Zhang and Zhang[9] employed a time-dependent technique to

[a]Present address: Fakultät für Physik, Universität Freiburg, D-79104 Freiburg, Germany.
[b]Present address: Steacie Institute for Molecular Sciences, National Research Council of Canada, Ottawa, Ontario K1A 0R6, Canada.

 0021-9606/94/101(6)/4759/10/$6.00

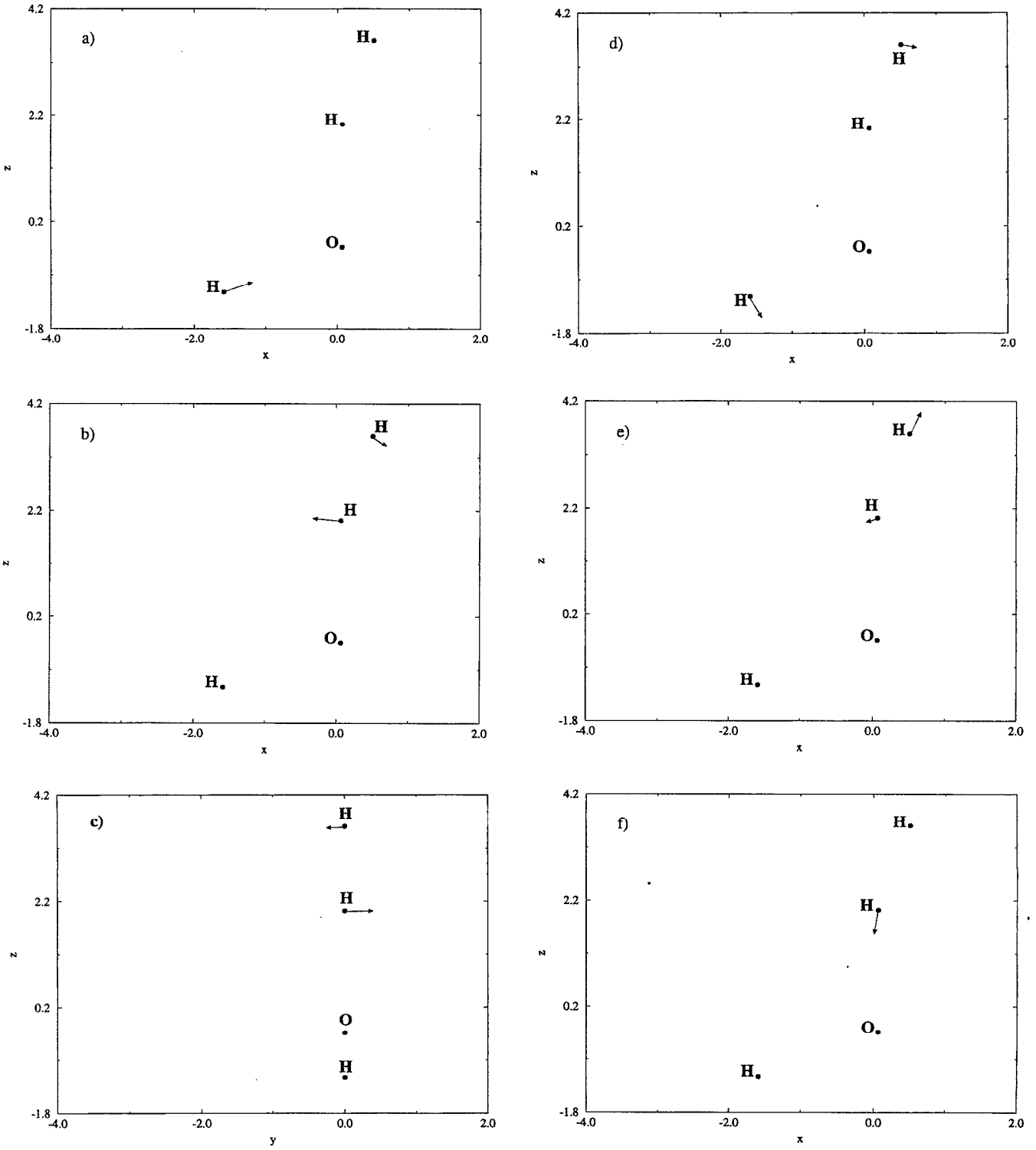

FIG. 1. Atomic displacements for motion along the six normal mode coordinates of the H_2+OH saddle point. (a)–(f) correspond to Q_1–Q_6, arranged as in Table I. The Cartesian x and z coordinates define the plane of the transition state. The arrows are drawn to scale.

investigate initial state-selected reaction probabilities for the $H_2+OH \rightarrow H+H_2O$ reaction. The reactant asymptotic region was included exactly, so that reaction probabilities for a given initial (vibrational and rotational) state could be calculated. Five degrees of freedom were included in their calculation, neglecting only the OH vibration. Within this approximation they reported reaction probabilities for a set of vibrationally and rotationally excited H_2 and rotationally excited OH initial states.

As noted above, our interest is the direct (but *correct*, i.e., without approximations) calculation of the CRP of Eq. (11). Seideman and Miller[16–18] developed a practical scheme

TABLE I. Frequencies and grid parameters.

Coordinate	Frequency (a.u.)	Number of grid points $E<0.2$ eV	$0.2\ \text{eV}\leq E\leq 0.4$ eV	$E>0.4$ eV
Q_1	0.016 153	4	4	4
Q_2	0.003 907	4	5	6
Q_3	0.003 781	5	5	7
Q_4	0.002 607	4	4	6
Composite grid		71 389	89 017	216 363

to perform such calculations. (One should also note other related approaches that deal with the flux–flux time correlation function.[19]) Their approach requires the use of some basis set (or grid) to represent the Hamiltonian in the transition state region of the potential energy surface. The CRP is expressed in terms of a modified Green's function $[E-(\hat{H}-i\hat{\epsilon})]^{-1}$, where ϵ is an absorbing potential at the edge of the grid that imposes outgoing wave boundary conditions for the Green's function. The numerical grid for such calculations is considerably smaller than for a full scattering calculation, resulting in considerably less computational effort for the rate calculation than for a complete state-to-state calculation.

The original formulation of the direct CRP calculation[17,18] involved the solution of a system of equations with a large number of right-hand side vectors: the action of the Green's function on each grid point in the reactant absorbing strip had to be computed. More recent work[20] has circumvented this difficulty: a Hermitian reaction probability operator was introduced which was shown to have only a small number of nonvanishing eigenvalues. These eigenvalues, which have shown to lie between 0 and 1, can be viewed as the rigorous generalization of the transmission probabilities of the transition state theory. The cumulative reaction probability is simply the sum of the eigenvalues of the reaction probability operator. A efficient iterative scheme for calculating the eigenvalues of the reaction probability operator was also presented. Again a set of a linear equations has to be solved, but compared to the original formulation[17,18] the number of right-hand side vectors, and therefore the computational effort, is drastically reduced. Now not the number of grid points in the reactant absorbing strip but the number of nonvanishing eigenvalues of the reaction probability operator determines the number of right-hand sides in the system of equations to be solved.

This article is organized as follows. In Sec. II the general methodology is reviewed and the numerical details are presented. Section III shows results for the cumulative reaction probability for vanishing total angular momentum ($J=0$). These results are used to calculate to thermal reaction rate as described in Sec. IV. Comparison to experimental data and to theoretical results of reduced dimensionality calculations is given. In Sec. V aspects of reduced dimensionality treatment are discussed extensively. Series of five-dimensional, four-dimensional, three-dimensional, and two-dimensional calculations are presented and compared to the full-dimensional result. Errors induced by the different reduced dimensionality models are analyzed.

II. CALCULATION OF $N(E)$

Following the approach developed by Seideman and Miller[17,18] and Manthe and Miller[20] the cumulative reaction probability is computed as

$$N(E)=\mathrm{tr}[\hat{P}(E)]=\sum_k p_k(E), \tag{4}$$

where $\hat{P}$ is the reaction probability operator, defined by

$$\hat{P}(E)=4\sqrt{\epsilon_r}\hat{G}(E)^{\dagger}\epsilon_p\hat{G}(E)\sqrt{\epsilon_r}, \tag{5}$$

and $p_k(E)$ are its eigenvalues, the eigen reaction probabilities. The Green's function

$$\hat{G}(E)=[E-(\hat{H}-i\hat{\epsilon})]^{-1} \tag{6}$$

involves the Hamiltonian operator of the molecular system, and $\hat{\epsilon}=\hat{\epsilon}_r+\hat{\epsilon}_p$ is an absorbing potential, $\epsilon_r(\epsilon_p)$ being the part in the reactant (product) region.

Normal coordinates of the transition state are employed which results in a Watson form of the Hamiltonian.[21] In the present work we limit attention to zero total angular momentum and neglect vibrational angular momentum terms, since they were seen in earlier work[18] to have negligible effect, which is expected be also the case here. The resulting Hamiltonian reads

$$\hat{H}=\sum_{n=1}^{6}-\frac{\hbar^2}{2}\frac{\partial^2}{\partial Q_n^2}+V(Q), \tag{7}$$

where Q_n are the mass-weighted normal coordinates of the six vibrational modes at the transition state. These normal coordinates are depicted in Fig. 1. Q_1 is best characterized as an O–H stretching mode. Q_2 describes mainly an in-plane H_2 rotation with approximately unchanged OH position, while Q_3 is the analogous out-of-plane motion. H_2–OH bending, or a simultaneous H_2 and OH rotation, is given by Q_4. The coordinates Q_5 and Q_6 are most strongly influenced by the reactive rearrangement. Q_5 is the H_2 stretch mode and coordinate Q_6 represents the motion of the H_2 hydrogen atom towards OH. Harmonic analysis at the transition state geometry results in real frequencies for the coordinates Q_1 to Q_5, while an imaginary value is found for the reaction coordinate Q_6. The frequencies are displayed in Table I. The potential $V(Q)$ is taken from the Schatz–Elgersma fit[14] to *ab-initio* results of Walch and Dunning[15] which was employed also in previous calculations of the H_2+OH→H+H_2O reaction.[6–9]

Discrete variable representations (DVR)[22,23] are used for the representation of the Hamiltonian and the absorbing potentials. A Gauss–Hermite DVR is employed in the coordinates Q_1 to Q_4. Depending on the specific coordinate and energy four to seven grid points per coordinate are required to reach convergence. For the reaction coordinate Q_6 and the Q_5 coordinate which is strongly coupled a sinc-function DVR[23] is employed. The grid spacing is chosen to allow for a maximum kinetic energy of 2.2 eV. The composite 6D grid

TABLE II. Parameters for absorbing potentials.

c_1	c_2	λ	q_0	q_{max}
0.375	0.625	1.5 eV	18 a.u.	37 a.u.

is truncated at a potential cutoff of 2.2 eV. The final grid consist of about 100 000 points for lower energies up to about 200 000 points for higher energies. More details are given in Table I.

The absorbing potentials are taken as functions of the two strongly coupled degrees of freedom, Q_5 and Q_6, and defined as follows:

$$\epsilon_p(q)=\begin{cases}0, & \text{for } q<q_0\\ \lambda\dfrac{(q-q_0)^4}{(q_{max}-q_0)^4}, & \text{for } q>q_0,\end{cases}$$

$$\epsilon_r(q)=\epsilon_p(-q), \tag{8}$$

where

$$q=c_1Q_5+c_2Q_6. \tag{9}$$

Only the part of the surface for $-q_{max}<q<q_{max}$ is included in the description. The parameters are given in Table II. The results obtained with these parameters are stable, and should be accurate, to at least 10% for all but the lowest energies ($E<0.05$ eV) reported.

As can be seen from the above description, a number of parameters must be adjusted in the calculation. Elaborate adjustment of each parameter in a full six-dimensional calculation of $N(E)$ would clearly be prohibitive because of the extreme computational effort of such calculations. Therefore the following scheme was employed. First two-dimensional calculations including only the coordinates Q_5 and Q_6 were performed for a set of total energies E. The parameters λ, q_0, and q_{max} were adjusted by systematic parameter variation in these calculations. Since the numerical effort of two-dimensional calculations is comparatively small, a large numbers of calculations can be performed easily. Next the kinetic and potential energy cutoffs employed in the definition of the DVR grid were likewise obtained from two-dimensional calculations. The number of DVR-grid points required in the other four coordinates Q_1 to Q_4 was determined by three-dimensional calculations. For each of these coordinates calculations including the coordinates Q_5,Q_6, and the coordinate in question were performed and the number of DVR-grid points in the coordinate in question is increased until convergence was achieved. It should be noted that the number of DVR-grid points required depends on the total energy E. Therefore this procedure was repeated for different energy regions. Finally a few full six-dimensional calculations were performed for different sets of parameters to ensure that the parameter values were sufficient also for the full calculation.

The eigenvalues p_k of the reaction probability operator $\hat{P}$ were calculated by the Lanczos scheme described in Ref. 20. Starting from a random initial vector ψ_0 a Lanczos-iteration sequence including reorthogonalization

$$\psi_n=\hat{P}\psi_{n-1}-\sum_{k=0}^{n-1}\psi_k\langle\psi_k|\hat{P}|\psi_{n-1}\rangle \tag{10}$$

is used to generate a orthonormal basis spanning the Krylov space $\{\psi_0,\hat{P}\psi_0,\hat{P}^2\psi_0,\ldots,\hat{P}^n\psi_0\}$. The representation of $\hat{P}$ within the basis $\{\psi_0,\psi_1,\ldots,\psi_n\}$ is then used to calculate the p_k's by direct numerical diagonalization. $N(E)$ is calculated directly by summing the diagonal elements

$$N(E)=\sum_{k=0}^{n}\langle\psi_k|\hat{P}|\psi_k\rangle. \tag{11}$$

The order n of the scheme is taken sufficiently large to yield converged results. At low energies 3 to 4 iterations are sufficient for this purpose while for the highest energies the required iterations increases up to 44.

The symmetry of the H_2 reactant in the H_2+OH→H+H_2O reaction causes a degeneracy of the eigen reaction probabilities p_k. The reaction can proceed equivalently in two ways: The OH can attack either the one side of the H_2 or the other. At the energies under consideration these two pathways do not interfere with each other. The normal coordinates employed here are constructed so that only one of the two pathways is explicitly included in the calculation. Therefore only one of each two degenerate p_k's is obtained. To account for the second set of p_k's the resulting $N(E)$ of Eq. (8) is multiplied by two.

Every action of the reaction probability operator $\hat{P}$ on a vector employed in the Lanczos iteration sequence requires two operations of the Greens function $\hat{G}$ (or its Hermitian conjugate) on a vector, or equivalently, the solution of two complex systems of linear equations of the form

$$\hat{A}x=f, \tag{12}$$

where in the present case

$$\hat{A}=E-(\hat{H}-i\epsilon)=\hat{G}(E)^{-1}, \tag{13}$$

and

$$f=\psi,\quad x=\hat{G}(E)\psi. \tag{14}$$

Given the size of basis involved in a six-dimensional problem, a direct solution, which requires storage of the Hamiltonian matrix in the core memory of the computer, is not feasible. Moreover, direct methods scale in time roughly as the cube of the order of the linear system and hence become prohibitively expensive as the dimensionality increases. Iterative methods do not require storage of the matrix and are particularly efficient for the case of sparse matrices which arise from discrete variable representations.

A variety of iterative methods for solving linear systems exists, a number of which are, at least in principle, applicable also to complex problems. In the present work we extended the generalized minimal residual (GMRES) algorithm, proposed by Saad and Schultz,[24] to the case of a general complex matrix. GMRES can be considered as a generalization of the minimal residual (MINRES) method[25] to nonsymmetric systems. It is based on application of the Arnoldi process[26] to compute an l_2-orthonormal basis of the Krylov subspace $K_k=v_1,Av_1,\ldots,A^{k-1}v_1$, where the initial vector

v_1 is a normalized residue, $v_1=(f-Ax_0)/\|(f-Ax_0)\|$, x_0 is an initial guess for the solution vector x, and k numbers the iterations. In this representation the system is upper Hessenberg and hence inexpensive to solve. Saad and Schultz[24] proposed a solution which minimizes the residual norm over K_k, by analogy to the MINRES method. In the present work we extended the algorithm of Ref. 24 to the case of a complex matrix and implemented it with a preconditioning matrix, as suggested in Refs. 27. Equation (12) is thus replaced by

$$\hat{B}^{-1}\hat{A}x=\hat{B}^{-1}f, \tag{15}$$

where the preconditioner B is chosen to be as similar as possible to A (so as to minimize the number of iterations by operating with a matrix $\hat{B}^{-1}\hat{A}$ that is similar to unity) but such that $\hat{B}^{-1}$ is easy to compute. Several preconditioners were tested and found to improve the performance of the method to various degrees. These include a separable and an adiabatic two- and three-dimensional approximations to the Hamiltonian and a diagonal preconditioner $B=\text{diag}\,A$. Extensive comparisons found the optimal preconditioner to be the simple diagonal matrix, consisting of the diagonal elements of A. The other more sophisticated (but more expensive to apply) preconditioners were found to reduce the number of iterations but result in an overall increase in the computational time as compared to the diagonal preconditioner. We stress, however, that this result is problem dependent, namely, it depends on the structure of the Hamiltonian matrix and hence on the choice of coordinate system. Particular care was taken to fully exploit the sparsity of the Hamiltonian as fully as possible by rearranging the matrix repeatedly so as to perform only nonzero multiplications. In the course of this work we tested several alternative iterative methods that are adaptable to complex systems, including a variation of Davidson's method[28] and the generalized conjugate Gradient algorithm.[29] We found GMRES to outperform these methods. This finding is to a certain extent also problem dependent, namely it depends on the desired accuracy and on the availability of an initial guess. We expect it to hold more generally in calculations of the Green's matrix, however, regardless of the precise structure and dimensionality of the Hamiltonian. Most of the comparisons of different algorithms were performed for the H+H_2 reaction, using normal mode coordinates as discussed in Ref. 18, and for reduced dimensionality versions of the H_2+OH problem.

III. RESULTS FOR H_2+OH→H+H_2O

Figure 2 displays the cumulative reaction probability for zero total angular momentum ($J=0$) as a function of the total energy. The zero of energy is chosen to be the energy of the reactants H_2 and OH in their respective ground state, i.e., including zero point vibrational energy. One interesting observation, in contrast to the findings for simple three-atom reactions, is that there is no remnant of the staircase structure predicted by classical transition state theory. This difference in behavior results from the increased number of degrees of freedom in the four-atom reaction H_2+OH→H+H_2O and can be understood by examining the different eigen reaction probabilities p_k, displayed in Fig. 3. As pointed out in earlier

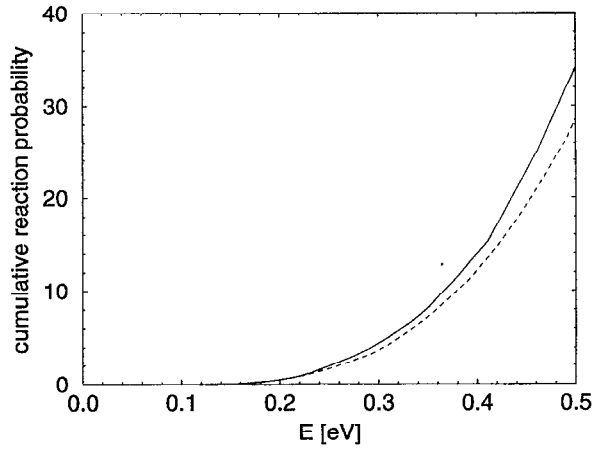

FIG. 2. Cumulative reaction probability $N(E)$ for $J=0$: present full dimensional calculation (full line), 3D calculation of Refs. 6 and 30 (dotted line), and experiment (crosses).

work[20] the p_k's can be interpreted as the contributions of the different states of the activated complex to the cumulative reaction probability. Figure 3 shows that all p_k's increase from 0 to 1 with increasing energy, but before an individual p_k has even nearly reached its final value the next p_k has already gained a considerable value. The different p_k contributions to $N(E)$ are thus overlapping, resulting in a smoothly increasing structure for $N(E)$.

The dotted line in Fig. 2 displays approximate results for $N(E)$ calculated by Wang and Bowman.[6,30] In this treatment all radial coordinate are included exactly, while all angular coordinates are treated by an adiabatic approximation. The description of the angle-type coordinates employs a harmonic approximation for the angular potential. The agreement with the full 6D results is quite good. At higher energies the approximate values tend to be too small. This deviation is explained easily. The approximate results assume harmonic potentials for the angular motion, while the real potentials are anharmonic. Therefore the energy of states which show excitation in an angular coordinate is too high in

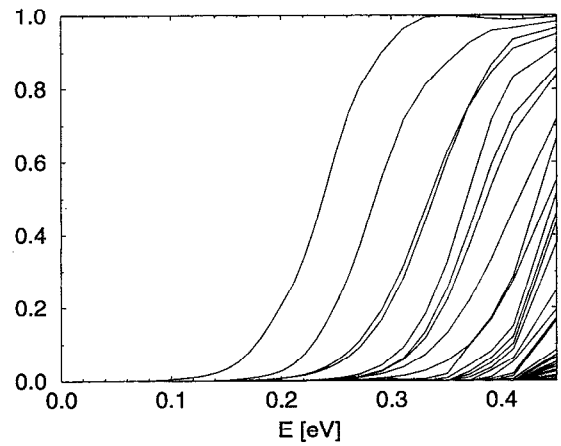

FIG. 3. Eigen reaction probabilities $p_k(E)$ for $J=0$.

the approximate description. Consequently, the total density of states, and also $N(E)$, is too small at a given energy E. Since the harmonic approximation becomes less accurate for higher excited states, the deviations can be expected to increase with increasing energy as observed in Fig. 2.

IV. THERMAL RATE CONSTANT

The thermal rate constant is the quantity which is observed in experiment, and it is given by the Boltzmann average of the cumulative reaction probability

$$k(T)=\frac{1}{2\pi\hbar Q_r(T)}\int_0^\infty e^{-E/kT}N_{\mathrm{tot}}(E)dE. \tag{16}$$

Here $N_{\mathrm{tot}}(E)$ is the total cumulative reaction probability,

$$N_{\mathrm{tot}}(E)=\sum_J (2J+1)N_J(E), \tag{17}$$

where $N_J(E)$ is the cumulative reaction probability for a total angular momentum J and Q_r is the partition function of the reactants. Assuming separability of vibrational and rotational motion at the transition state (the "J shifting"[31] or modified wave number[32] approximation) each $N_J(E)$ can be calculated by shifting the $J=0$ value by the appropriate rotational energy

$$N_J(E)=\sum_{K=-J}^{J} N_{J=0}(E-E_{\mathrm{rot}}^{JK}). \tag{18}$$

E_{rot}^{JK} is the rotational energy of the activated complex with the J,K-rotational quantum numbers. Inserting Eqs. (17) and (18) in Eq. (16) yields

$$k(T)=\frac{Q_{\mathrm{rot}}^{\neq}(T)}{2\pi\hbar Q_r(T)}\int_0^\infty e^{-E/kT}N_{J=0}(E)dE, \tag{19}$$

where $Q_{\mathrm{rot}}^{\neq}$ is the rotational partition function of the activated complex. Within the parameter range under consideration it can be well approximated by its classical limit

$$Q_{\mathrm{rot}}^{\neq}(T)=\hbar^3\sqrt{\frac{\pi(kT)^3}{8I_AI_BI_C}}, \tag{20}$$

where I_A, I_B, and I_C are the three principle moments of inertia of the activated complex.

The reactant partition function $Q_r(T)$ consists of contributions from the vibrational and rotational motion of the H_2 and OH reactant molecules and from their relative translational motion. For OH an electronic contribution

$$Q_{\mathrm{OH}}^{\mathrm{elec}}(T)=1+e^{-\Delta E_{\mathrm{elec}}/kT} \tag{21}$$

($\Delta E_{\mathrm{elec}}=140\ \mathrm{cm}^{-1}$) is included. It results from the spin-orbit splitting of the $^2\Pi$ ground state of OH. Since only one of these electronic states correlates to the activated complex, no multiplying factors due to electronic degeneracy (or near degeneracy) are included.

Before presenting calculated rate constants for the $H_2+OH\rightarrow H+H_2O$ reaction a problem of the potential energy surface employed has to be mentioned. The potential energy surface was constructed by Schatz and Elgersma[14] as a fit to the *ab initio* results of Walch and Dunning.[15] However, the geometry of the transition state given by the Schatz–Elgersma-fit differs significantly from the original Walch and Dunning transition state geometry. Therefore, two sets of moments of inertia of the activated complex can be used alternatively in Eq. (20): the Schatz–Elgersma-surface results in $I_A=4079$ a.u., $I_B=37\,520$ a.u., $I_C=41\,599$ a.u., while the Walch and Dunning data gives $I_A=983$ a.u., $I_B=42\,288$ a.u., $I_C=43\,270$ a.u. $Q_{\mathrm{rot}}^{\neq}$ values derived from these moments of inertia are smaller by a factor of about 0.5 for the Walch and Dunning data compared to the Schatz and Elgersma fit. To be consistent in the treatment of internal and rotational motion, rotational constants corresponding to the Schatz–Elgersma fit are used throughout the present work. This should enable comparison to other theoretical work, where the overall rotational motion was not approximated as separable. Analogous results employing the Walch–Dunning geometry can be obtained by multiplying the rates presented below by a factor of 0.53.

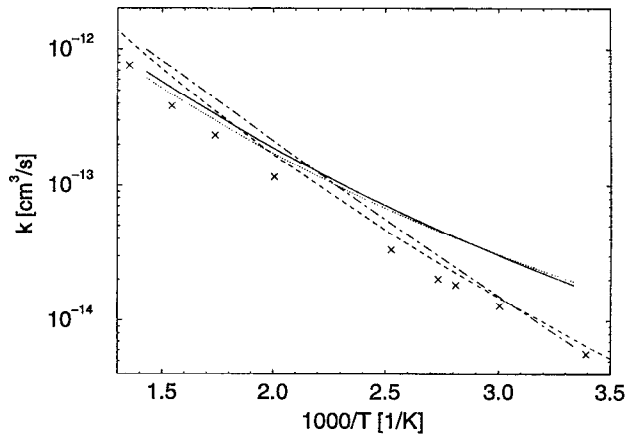

FIG. 4. Thermal rate constant $k(T)$: present full dimensional calculation (full line), 3D calculation of Refs. 6 and 30 (dotted line), rotating bound approximation results (Ref. 7) (dashed line), present three-dimensional approximation (dash–dot line), and experiment (crosses).

The rate constant calculated using Eq. (16) is shown as the solid curve in Fig. 4. The energy range considered allows calculation of the rate constant for temperatures between 300 and 700 K. For lower temperatures energies below 0.05 eV contribute and for higher temperatures energies above 0.5 eV would have to be included. The experimental reaction rates[12] are indicated by crosses in Fig. 4. One sees that the calculated reaction rate is larger than the experimental one, and that it decreases more slowly with increasing $1/T$ than the experimental one. We do not believe that the J-shifting approximation can be this much in error at these relatively low energies, so the conclusion is that this lack of agreement is due to inaccuracies in the potential energy surface.

Independent of agreement with the experimental data, the results of the full-dimensional calculation are interesting for comparison with approximate calculations. There have been a number of reduced dimensionality quantum calculations of the $H_2+OH\rightarrow H+H_2O$ reaction based on the Schatz–Elgersma surface. The Wang and Bowman[6,30] calcu-

lation mentioned earlier is displayed in Fig. 2. The corresponding reaction rate, computed within the J-shifting approximation, is displayed as dotted line in Fig. 4. The deviation from the full-dimensional calculation is quite small, the somewhat weaker temperature dependence follows from the approximate topology of the surface, discussed in Sec. III.

Clary[7] studied the H_2+OH reaction in a different reduced dimensionality calculation where the system is constrained to planar geometry and the H_2 rotation as well as the OH stretching is frozen. The resulting reaction rate is displayed in Fig. 4 as a dashed line. Clary's rate decreases less strongly with increasing $1/T$ than the full-dimensional result. It is in better agreement with experiment than the exact full-dimensional calculation, but we believe that this agreement is fortuitous (see below).

To get more insight into the effects of reduced dimensionality approximation, reduced dimensionality calculations based on the normal coordinates employed in this work were performed. Details are described in Sec. V. For comparison with Clary's results $k(T)$ was calculated including only the normal coordinates Q_4, Q_5, and Q_6. This set of normal coordinates resembles most closely the set of Jacobi-type coordinates employed in Clary's work. The resulting reaction rate is displayed in Fig. 4 as dash-dotted line. The difference from Clary's result is rather small, especially the temperature dependence is very similar. This suggests that the deviation between Clary's calculation and the present full-dimensional one results from the neglect of three internal degrees of freedom in Clary's calculation and not from a failure of the J-shifting approximation invoked in the full-dimensional calculation. We conclude that Clary's calculation is less accurate than the present one for the given potential energy surface but cancellation of errors produces better agreement of his results with experiment.

V. EFFECTS OF DIMENSIONALITY

The previous section has demonstrated that theoretical results for the H_2+OH→H+H_2O reaction rate depend sensitively upon how the different degrees of freedom are taken into account. Many theoretical studies of reaction dynamics, especially in larger systems, are based on models where motion in several degrees of freedom is neglected or treated adiabatically. Since such approximations will remain essential, it is important to investigate their effect. To this end we have tested several reduced dimensionality models.

Though one expects such "reduced dimensionality" approximations to work best if local mode (or bond) coordinates are used, it may often be the case for complex systems that one will have only a normal mode description of the transition state region. Thus our reduced dimensionality calculations are defined in terms of normal coordinates, assuming motion in different sets of these coordinates to be separable. These separable coordinates are described in a harmonic approximation employing the frequency at the transition state geometry. The reduced dimensionality reaction probability is calculated employing the remaining coordinates as described in Sec. II for the full-dimensional problem. For example, if motion in the OH stretch-type normal

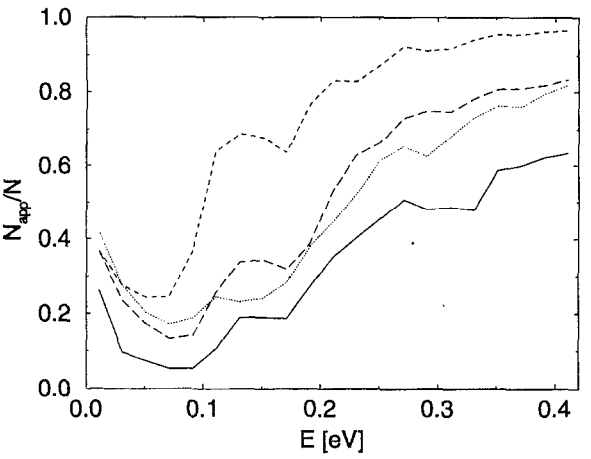

FIG. 5. N_{app}/N ratio as a function of energy for different five-dimensional approximations. Modes being separated are Q_1 (full line), Q_2 (long dashed line), Q_3 (dashed line), and Q_4 (dotted line).

coordinate Q_1 is assumed to be separable, a reduced dimensionality cumulative reaction probability $N_{5D}(E)$ is calculated employing a Hamiltonian where the Q_1 coordinate is frozen at its equilibrium value $Q_1=0$. The Q_1 mode is then convoluted in the usual microcanonical fashion to produce the approximate cumulative reaction probability for the full system,

$$N_{app}(E)=\sum_{n_1} N_{5D}[E-\hbar\omega_1(n_1+\tfrac{1}{2})]. \tag{22}$$

Analogous procedures are employed when separability of other degrees of freedom is assumed. The ratio of such approximate cumulative reaction probability to the exact full-dimensional one, $[N_{app}(E)/N(E)]$, is used to measure the accuracy of the approximative treatment.

In the calculations presented below separability of different sets of the coordinates Q_1 to Q_4 will be investigated. Since the coordinate Q_5 is strongly coupled to the reaction coordinate Q_6, nonsensical results are obtained if it is assumed to be uncoupled. Thus all calculations below include at least two degrees of freedom fully coupled, with the remaining uncoupled ones convoluted microcanonical to obtain the approximate $N(E)$ (all for $J=0$).

Figure 5 displays N_{app}/N as a function of energy for various 5D calculations, i.e., where only one of the coordinates is assumed to be separable and harmonic. It is immediately seen that this approximation yields significant errors independent of the actual coordinate which is treated as being separable. Deviations are especially strong in the tunneling regime. There the approximate cumulative reaction probability is lower by a factor of up to 20 compared to the exact 6D result. Due to the exponential dependence of $N(E)$ on the energy in this regime, even minor errors in the potential induced by the separability approximation result in crucial errors in the cumulative reaction probability. Since the assumption of separability and harmonicity tends to overestimate the potential energies, the approximate cumulative reaction probabilities are too small. For higher energies $N(E)$, where

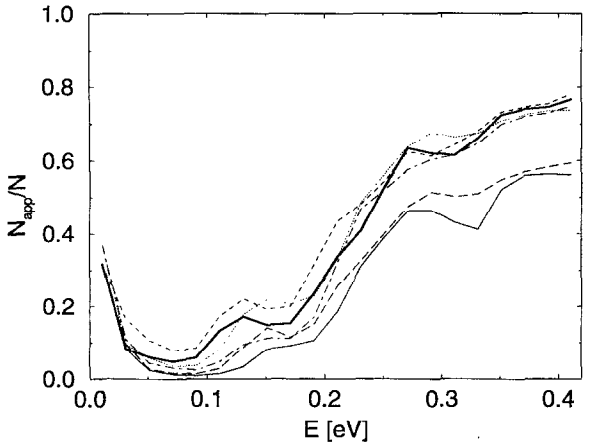

FIG. 6. N_{app}/N ratio as a function of energy for different four-dimensional approximations. Modes being separated are Q_1 and Q_2 (full line), Q_1 and Q_3 (long dashed line), Q_1 and Q_4 (dashed line), Q_2 and Q_3 (dotted line), Q_2 and Q_4 (dash–dot line), and Q_3 and Q_4 (thick full line).

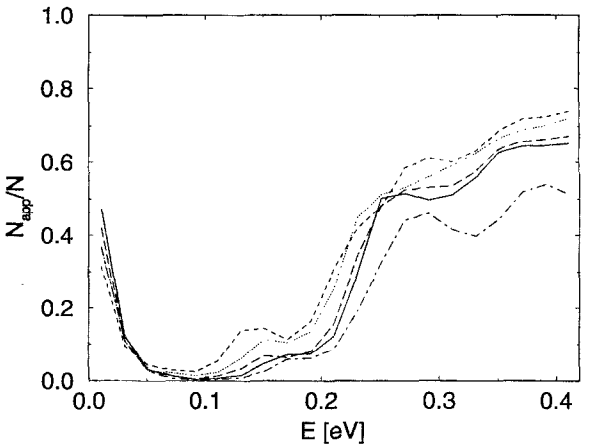

FIG. 7. N_{app}/N ratio as a function of energy for different three-dimensional approximations. Modes included in the exact calculation are Q_5, Q_6 and the following one: Q_1 (long dashed line), Q_2 (dashed line), Q_3 (dotted line), and Q_4 (dash–dot line). The full line indicates the two-dimensional result where only Q_5 and Q_6 are included exactly.

more states of the activated complex contribute to $N(E)$, the precise energies of individual states are no longer of such crucial importance, and the deviation of $N_{app}(E)$ from $N(E)$ decreases with increasing energy. But even for the highest energies under consideration errors can be significant. In Fig. 5 the N_{app} are to low by 20% to 50% for three of the four cases studied.

So far general trends have been discussed. We now consider the effect of assuming separability of individual vibrational modes and the immediate findings are rather surprising. Separating (i.e., assuming separability for) the vibrational mode Q_1, which describes O–H stretching motion, shows a larger effect on the results than separating any other mode; even at the highest energies under consideration N_{app} barely reaches above 50% of the exact $N(E)$. These findings are in apparent contradiction to the assumptions utilized in previous work on the H_2+OH→H+H_2O reaction[7,8] where the O–H stretching motion is assumed to be the least important degree of freedom. However, care has to be taken in such comparisons, since in the present study normal coordinates are employed while previous work was typically been based on Jacobi-type coordinates. This will be discussed more comprehensively below when the 4D results are presented.

Separating the out-of-plane motion (Q_3) results in the smallest error. While discrepancies remain large in the tunneling regime even in this case, high energy results for N_{app} are in quite good agreement with the exact values; above 0.3 eV errors are less than 10%. Therefore treating the reaction as occurring in planar geometry seems to be a good approximation when studying activated H_2+OH→H+H_2O reaction processes. Motion in the other two modes Q_2 and Q_4 is more strongly coupled to the reaction process, yielding significant errors of above 20% even in the activated regime.

Figure 6 shows N_{app}/N ratios for various 4D calculations, i.e., when two coordinates are approximated as separable. The general appearance of the curves is similar to the findings of Fig. 5. In the tunneling regime N_{app} is much too small, but even for higher energies the approximate values are significantly too low. Two different sets of curves can be distinguished. If the coordinate combinations Q_1/Q_4, Q_2/Q_4, Q_3/Q_4, and Q_2/Q_3 are approximated as separable, the resulting errors are significantly smaller than for the combinations Q_1/Q_2 and Q_1/Q_3. In other words, if the coordinate Q_1 is separated then also Q_4 has to be separated to avoid large errors. This is consistent with the findings of Fig. 5 where separating only the Q_1 mode was found to result in especially large errors. The definition of the normal coordinates as displayed in Fig. 1 gives the key to the explanation. Q_1 describes mainly OH stretching motion, while the rotation of the OH group is primarily described by the coordinate Q_4. However, associating the normal coordinates with stretching or rotational motion is correct only for small displacements from the reference geometry. Actual rotation of the OH group changes the values of Q_4 and Q_1. While OH stretching motion is generally assumed to be not very important in the reaction process, OH rotation is important. Separating Q_1 and assuming a harmonic potential for this coordinate therefore hinders the OH rotation and results in too small values for N_{app}. To keep the treatment balanced one has to separate also the Q_4 mode in which case Q_4 mimics the rotational-type motion by low frequency vibrational motion.

Finally, Fig. 7 shows the result of various 3D calculations, i.e., N_{app}/N ratios obtained when three modes are approximated as separable. Differences compared to Fig. 6 are rather small, especially for higher energies. For lower energies the reaction rates are further decreased which is easily explained by the above arguments. Results are rather independent of which coordinates are separated. Only when all coordinates except Q_4 are separated, N_{app}/N becomes considerably smaller than for any other combination. This finding is in agreement with results of Fig. 5 and Fig. 6: if Q_1 is treated as separable larger errors are caused unless Q_4 is also approximated as separable.

The N_{app}/N ratio for a the 2D calculation, including only Q_5 and Q_6 exactly, is also shown in Fig. 7. Differences from the 3D results are small, especially if the Q_1 coordinate is the third coordinate in the three-dimensional calculation. This implies that a simple minded investigation starting from 2D calculations and proceeding to higher dimensional ones could easily draw wrong conclusions. Since the 3D result which includes the Q_1 coordinate is not very different from the 2D result, the Q_1 coordinate could be judged to be unimportant and consequently be dropped. Figure 5, however, shows that Q_1 has the largest effect when changing from a full dimensional to a five-dimensional calculation! This demonstrates that correlation between motions in different modes can be important (at least when using normal coordinates). Therefore care has to be taken in judging the importance of different coordinates in reduced dimensionality studies.

VI. CONCLUSIONS

An exact quantum, full-dimensional calculation of the ($J=0$) cumulative reaction probability for the $H_2+OH \rightarrow H+H_2O$ reaction has been presented. From this data the reaction rate is calculated for temperatures between 300 and 700 K.

This calculation is of interest for several reasons. First, it demonstrates that the technique developed in Refs. 17 and 18 and Ref. 20 allows for efficient calculations of cumulative reaction probabilities and reaction rates for larger systems. Calculating these quantities for a four-atom reaction including all six internal degrees of freedom is demonstration of the power of this approach. To the best of our knowledge there have been no other exact quantum calculation of the cumulative reaction probability on a such a system up to now.

When reaction rates are calculated by an exact full quantum method the only remaining source of errors is generally the potential energy surface employed. Therefore comparison to experimental rates provides an unambiguous test of the quality of the surface. In the example presented here reaction rates derived from the Schatz–Elgersma surface[14] for the $H_2+OH \rightarrow H+H_2O$ reaction showed significant deviations from the experimental rates. Improvement of this surface thus appears to be necessary in order to obtain a quantitative description of this reaction.

Clearly the range of systems for which exact full-dimensional calculations are feasible is limited. Even for the $H_2+OH \rightarrow H+H_2O$ reaction, which is a rather simple example of a four-atom reaction, the numerical effort of the full-dimensional calculation presented here is considerable: On an up to date workstation a few weeks of CPU time are required to compute the results presented. Therefore the development of approximate treatments is an important issue. But availability of exact reaction rates for a given potential energy surface is important, at least to serve as a reference when judging the quality of approximate results. As an example of the investigation of approximate treatments, reduced dimensionality treatments have been investigated in this work. Comparison to reduced dimensionality calculation of other authors as well as a systematic study of normal coordinate based reduced dimensionality calculation have been presented. The findings indicates that correlation between motion in different normal coordinates can be important. In the present case, this results in a strong effect of the OH stretching type normal coordinate. Out-of-plane motion of the activated complex is found to be the least important degree of freedom.

ACKNOWLEDGMENTS

We would like to thank Professor J. M. Bowman for communicating his unpublished results (from work with Dr. D. Wang) for $N(E)$ and $k(T)$ and also very useful discussions. We thank Professor R. E. Wyatt for introducing us some years ago to the GMRES algorithm. This work has been supported by the Director, Office of Energy Research, Office of Basic Energy Science, Chemical Science Division of the U.S. Department of Energy under Contract No. DE-AC03-76SF00098 and also by the National Science Foundation under Grant No. CHE-8920690. U.M. acknowledges support from the Fond der Chemischen Industrie.

[1] U. Manthe, T. Seideman, and W. H. Miller, J. Chem. Phys. **99**, 10078 (1993).
[2] G. C. Schatz and A. Kuppermann, J. Chem. Phys. **65**, 4668 (1976); M. Mladenovic, M. Zhao, D. G. Truhlar, D. W. Schwenke, Y. Sun, and D. J. Kouri, *ibid.* **92**, 7035 (1988); J. Z. H. Zhang and W. H. Miller, *ibid.* **91**, 1528 (1989); J. M. Launay and M. Le Dourneuf, Chem. Phys. Lett. **163**, 178 (1989); D. E. Manolopoulos and R. E. Wyatt, J. Chem. Phys. **92**, 810 (1990); D. Neuhauser, R. S. Judson, D. J. Kouri, A. D. Adelman, N. E. Shafer, D. A. V. L. Kliner, and R. N. Zare, Science **257**, 519 (1992); A. Kupperman and Y. S. M. Wu, Chem. Phys. Lett. **205**, 577 (1993).
[3] J. M. Launay and M. Le Dourneuf, Chem. Phys. Lett. **169**, 473 (1990); D. Neuhauser, R. S. Judson, M. Baer, R. L. Jaffe, and D. J. Kouri, *ibid.* **176**, 546 (1991); J. Z. H. Zhang, *ibid.* **181**, 63 (1991).
[4] G. C. Schatz, Chem. Phys. Lett. **150**, 92 (1988).
[5] A. N. Brooks and D. C. Clary, J. Chem. Phys. **92**, 4178 (1990); Q. Sun and J. M. Bowman, *ibid.* **92**, 5201 (1990); Q. Sun, D. L. Yang, N. S. Wang, J. M. Bowman, and M. C. Lin, *ibid.* **93**, 4730 (1990).
[6] D. Wang and J. M. Bowman, J. Chem. Phys. **96**, 8906 (1992).
[7] D. C. Clary, Chem. Phys. Lett. **192**, 34 (1991); D. C. Clary, J. Chem. Phys. **95**, 7298 (1991); **96**, 3656 (1992).
[8] J. Echave and D. C. Clary, J. Chem. Phys. **100**, 402 (1994).
[9] D. H. Zhang and J. Z. H. Zhang, J. Chem. Phys. **99**, 5615 (1993); **100**, 2697 (1994).
[10] D. C. Clary and G. C. Schatz, J. Chem. Phys. **99**, 4578 (1993).
[11] J. Echave and D. C. Clary, J. Chem. Phys. **100**, 3556 (1994).
[12] F. P. Tully and A. R. Ravishankara, J. Phys. Chem. **84**, 3126 (1980); A. R. Ravishankar, J. M. Nicovich, R. L. Thompson, and F. P. Tully, *ibid.* **85**, 2498 (1981).
[13] A. Sinha, M. C. Hsiao, and F. F. Crim, J. Chem. Phys. **94**, 4928 (1991); M. J. Bronikowski, W. R. Simpson, B. Girard, and R. N. Zare, *ibid.* **95**, 8647 (1991); K. Kessler and K. Kleinermanns, Chem. Phys. Lett. **190**, 145 (1992); M. Alagia, N. Balucani, P. Casavecchia, D. Stranges, and G. G. Volpi, J. Chem. Phys. **98**, 2459 (1993).
[14] G. C. Schatz and H. Elgersma, Chem. Phys. Lett. **73**, 21 (1980).
[15] S. P. Walch and T. H. Dunning, J. Chem. Phys. **72**, 1303 (1980).
[16] W. H. Miller, J. Chem. Phys. **61**, 1823 (1974); W. H. Miller, S. D. Schwartz, and J. W. Tromp, *ibid.* **79**, 4889 (1983).
[17] T. Seideman and W. H. Miller, J. Chem. Phys. **96**, 4412 (1992).
[18] T. Seideman and W. H. Miller, J. Chem. Phys. **97**, 2499 (1992).
[19] R. E. Wyatt, Chem. Phys. Lett. **121**, 301 (1985); J. Jaquet and W. H. Miller, J. Chem. Phys. **89**, 2139 (1985); J. W. Tromp and W. H. Miller, *ibid.* **90**, 3482 (1986); T. J. Park and J. C. Light, *ibid.* **85**, 5870 (1986); G. Wahnström and H. Metiu, Chem. Phys. Lett. **134**, 531 (1987); D. Brown and J. C. Light, J. Chem. Phys. **97**, 5465 (1992); M. Thachuk and G. C. Schatz, *ibid.* **97**, 7297 (1992).
[20] U. Manthe and W. H. Miller, J. Chem. Phys. **99**, 3411 (1993).
[21] J. K. G. Watson, Mol. Phys. **15**, 479 (1968).
[22] D. O. Harris, G. G. Engerholm, and W. D. Gwinn, J. Chem. Phys. **43**, 1515 (1965); A. S. Dickinson and P. R. Certain, *ibid.* **49**, 4209 (1968) J. C.

Light, I. P. Hamilton, and J. V. Lill, *ibid.* **82**, 1400 (1985).
[23] D. T. Colbert and W. H. Miller, J. Chem. Phys. **96**, 1982 (1992).
[24] Y. Saad and M. H. Schults, SIAM J. Stat. Comput. **7**, 856 (1986).
[25] C. C. Paige and M. A. Saunders, SIAM J. Numer. Anal. **12**, 617 (1975).
[26] W. E. Arnoldi, Quart. Appl. Math. **9**, 17 (1951).
[27] See, for example, L. A. Hageman and D. M. Young, *Applied Iterative Methods* (Academic, New York, 1981); O. B. Axelsson, On Preconditioning and Convergence Acceleration in Sparse Matrix Problems, Technical Report CERN74-10, CERN, Geneva (1974), and references therein.
[28] E. R. Davidson, J. Comput. Phys. **17**, 87 (1975).
[29] See, for example, S. C. Eisenstat, H. C. Elman, and M. H. Schultz, SIAM J. Numer. Anal. **10**, 345 (1983); Y. Saad and M. H. Schults, Math. Comput. **44**, 417 (1985).
[30] J. M. Bowman and D. Wang (private communication).
[31] J. M. Bowman, J. Chem. Phys. **95**, 4960 (1991).
[32] K. Takayanagi, Prog. Theor. Phys. **8**, 497 (1952); E. E. Nikitin, *Elementary Theory of Atomic and Molecular Processes in Gases* (Oxford University, Oxford, 1974), pp. 58–60.